ORIGINAL ARTICLE

WILEY Xenotransplantation

Remission of hyperglycemia in spontaneously diabetic NOD mice upon transplant of microencapsulated human umbilical cord Wharton jelly-derived mesenchymal stem cells (hUCMS)

Pia Montanucci[1] | Teresa Pescara[1] | Alessia Alunno[2] | Onelia Bistoni[2] | Giuseppe Basta[1] | Riccardo Calafiore[1] (iD)

[1]Section of Cardiovascular, Endocrine and Metabolic Clinical Physiology, and Laboratory for Endocrine Cell Transplants and Biohybrid Organs, Department of Medicine, University of Perugia, Perugia, Italy

[2]Section of Rheumatology, Department of Medicine, University of Perugia, Perugia, Italy

Correspondence
Riccardo Calafiore, Department of Medicine, University of Perugia, Perugia, Italy.
Email: riccardo.calafiore@unipg.it

Abstract

Background: Our previous in vitro demonstration of the immunoregulatory effects of microencapsulated hUCMS on human peripheral blood mononuclear cells (PBMCs) extracted from patients with recent onset, type 1 diabetes mellitus (DM), prompted us to test our product for xenograft (TX) in non obese diabetic (NOD) mice with spontaneous DM.

Methods: We transplanted microencapsulated hUCMS into the peritoneal cavity of NOD mice with either severe or mild DM. Blood glucose (BG) levels were monitored following TX, in either basal or upon glucose stimulation.

Results: Only the NODs with mild DM showed full and sustained remission of hyperglycemia throughout 216 days post-TX, unlike recipients with severe DM, where no remission of hyperglycemia was attained, as reflected by erratic BG levels at all times.

Conclusions: These data suggest that the stage of DM disease process in NOD mice, reflecting steady decline of residual b-cell mass, plays a pivotal role in determining the success of this cell therapy approach for treatment of DM.

KEYWORDS
immunoregulation, microencapsulation, NOD mice, sodium alginate, stem cells, T1D

1 | INTRODUCTION

Type 1 diabetes (T1D) notoriously depends on selective autoimmune killing of pancreatic islet β-cells. For the past 25 years, attempts to identify the underlying mechanisms have been unsuccessful due to the polyclonal nature of this autoimmune disease, in conjunction with the wider challenges posed by immune regulation in T1D patients.[1,2]

Among potential cell therapy approaches for T1D, the use of human umbilical cord matrix stem cells (hUCMS) has recently gained growing interest. Briefly, hUCMS identify with post-natal adult stem cells, able to differentiate into several cell lineage phenotypes,[3] both in vitro and in vivo. Further clinical interest has

been fueled by the observation that hUCMS are immunoprivileged, due to both the lack of HLA class II antigens and intrinsic immunomodulatory properties.[4-6] These appear predominantly related to the production of humoral factors.[7-10] hUCMS also express the following three classes of HLA: HLA-E, HLA-F, and HLA-G. These molecules are involved in the tolerogenic process occurring at the fetal-maternal interface.[11] In particular, it has been recently described that HLA-G, released from human mesenchymal stem cells, may promote the expansion of Treg populations.[12]

Operative use of hUCMS, for clinical grafting procedures, has encountered, so far, a number of obstacles.[13] On one hand, graft of hUCMS adversely is affected by the complex disease scenario. Furthermore, hUCMS might result in undesired terminal cell phenotypes.[14] These issues could be avoided by the envelopment of hUCMS into special

---

G.B. and R.C. share senior co-authorship of this paper.

wileyonlinelibrary.com/journal/xen

microcapsules.[15] Toward this end, we have used, in our laboratory, our alginate-based microencapsulation technology.[16] This technique involves cell entrapment within polymeric artificial membranes that constitute biocompatible, selectively permeable and immunoprotective physical barriers.[17-19] The three-dimensional architecture of the microcapsules, based on highly purified and almost endotoxin- and protein-free alginates, resulted in excellent trans-membrane biochemical exchange. The microcapsule three-dimensional configuration promoted better growth, differentiation, and maturation of different cell types, including mesenchymal stem cells, mouse and human embryonic stem cells, and hepatocytes.[20] Recently, we have obtained preliminary evidence that microencapsulated hUCMS, pre-stimulated with IFN-γ, positively affected the immune system by both reducing pathogenic T-cell subsets and potentiating their regulatory counterparts. The pro-inflammatory cytokine IFN-γ induced expression of IDO1, a molecule involved in the tryptophan catabolism, and led to an increase in HLA-G5 expression: Both these molecules play a pivotal role in a number of immunoregulatory pathways.[21]

1.1 | Aim

The aim of this work was to verify whether microencapsulated hUCMS xenograft (TX) would enable normalization of blood glucose (BG), both in basal, and upon intraperitoneal glucose tolerance test (IPGTT), in non obese diabetic (NOD) mice with recent-onset diabetes. We also sought to determine whether the eventually restored normoglycemia would persist long term, and if so, whether this would link to a hUCMS-related immunomodulatory effect on regulatory T-cell subsets (Tregs), and to a hUCMS paracrine action on islet cells, thereby allowing for preservation of the mouse endocrine pancreatic morphology.

2 | MATERIALS AND METHODS

2.1 | hUCMS isolation procedure

The isolation procedure of hUCMS from the post-partum umbilical cord complied with an official consent from the University of Perugia Hospital Board and informed consent from patients. The cords, at term of gestation, upon retrieval, were soaked in PBS, supplemented with antibiotics on ice, and transported from the Section of Obstetrics and Gynecology, Department of Surgery, to our laboratory. Only those cords that were associated with an overall ischemia time of lower than 6 hours entered our protocol.[3] In brief, following washing, each cord was cut into 10-cm pieces that were sealed at both ends. A digestion solution, containing 1.25 mg mL^{-1} hyaluronidase (Sigma-Aldrich, Milano, Italy) and 1.5 mg mL^{-1} collagenase P (Roche, Milano, Italy), in 0.02 M phosphate buffer at pH 7, containing 77 mM NaCl and 0.01% BSA (Sigma-Aldrich), was injected into the cord segments (Wharton jelly). These were moved to a glass bottle, thereby agitated in a water bath at 37°C for 30 minutes. The tissue digest was centrifuged at 1500 rpm, for 5 minutes at 4°C, and re-suspended in DMEM (Gibco, Life Technology, Milano, Italy) with antibiotics. The cell suspension was spun on Lymphoprep™ gradients at 1850 rpm for 20 minutes at 4°C, and after washing, was plated. The cells were seeded at a concentration of 6000-8000 cells cm^{-2}, in CMRL medium (Biospa, Milano, Italy), supplemented with 10% fetal bovine serum (FBS; Biospa), 1% L-glutamine, and 1% penicillin/streptomycin (Biospa). The cells were maintained at 37°C in humidified 95% air. Cell expansion, until 80% confluence, was followed by treatment with 0.05% trypsin/EDTA (Gibco, Invitrogen, Milan, Italy) for 3 min at 37°C.

2.2 | Phenotypic analysis of hUCMS

To assess the mesenchymal nature of the isolated cells, the non-fixed tissue underwent flow cytometry analysis. The preparations were exposed to the following conjugated antibodies: integrin beta-1/CD29 antibody (MEM-101A), fluorescein isothiocyanate (FITC) conjugate; CD90/Thy-1 antibody (eBio5E10), FITC conjugate; CD105/Endoglin antibody (SN6), RPE conjugate; CD44/H-CAM antibody (IM7), PerCP-Cy5.5 conjugate; and CD45/PTPRC antibody (HI30), Pacific Orange conjugate, all from Molecular Probes. The cells were analyzed with the Attune® Acoustic Focusing Cytometer (Thermo Fisher Scientific). Ten thousand events were recorded per each condition.

2.3 | Differentiation protocols

Cells were examined for their adipogenic and osteogenic differentiation potentials. On this purpose, hUCMS were incubated in specific induction culture media as previously reported, for three weeks, and were stained with Oil-Red-O or with Alizarin Red-S, respectively.[3]

2.4 | Alginate (AG) procurement and purification for microencapsulation

We purchased powdered AG from Monsanto-Kelco and featured the following properties: molecular weight =120,000-190,000 kDa; mannuronic acid (M) and guluronic acid (G) = M fraction (F_M) 61%; and G fraction (F_G) 39% ("high M" blend). The alginate "ultrapurification" process was conducted in house, under GLP conditions, based on patent no. WO 2009093184 A1.[22] The final alginate preparation exhibited the following properties: (i) Endotoxin levels, as measured by LAL test, were <27.8 EU g^{-1} (<0.5 EU mL^{-1}) (any values below 100 EU g^{-1} in this test identify as "endotoxin-free"); (ii) protein content was <0.45%; (iii) viscosity was 100-300 cps; and (iv) heavy metal content was below the recommended cutoff, with the following values: Ca<100 ppm; Cu<40 ppm; Fe<60 ppm; Hg<40 ppb; Mg<40 ppm; Zn<40 ppm; Pb<50 ppm; Si<10 ppm; Mn<10 ppm; Sr<40 ppm; and As<100 ppb.

2.5 | Microencapsulation of hUCMS

Microencapsulation consists of entrapping live cells within polymeric and non-cytotoxic artificial membranes such as alginates that serve for immunoprotective barriers. Briefly, the cell pellets were mixed with 1.8% alginate solution, in order to make a final homogeneous alginate/cell suspension. The AG/hUCMS proportion was 1.3 mL

alginate/2.5×10^6 cells: This AG/cell ratio prevented the formation of empty capsules or capsules containing excessive cell numbers. The AG/cell suspension was then extruded through a microdroplet generator, under the combination of air shears with mechanical pressure; the alginate droplets were collected in a 1.2% $CaCl_2$ bath (Sigma-Aldrich), which immediately turned them into gel microbeads. The beads were sequentially coated with 0.12%, 0.06% poly-L-ornithine (Sigma-Aldrich), de-gelled with 55 mM sodium citrate, and finally covered with an outer coat of 0.06% ultrapurified alginate, so as to obtain biologically acceptable and functionally performing microcapsules.[16] Sterility and viability testing, the latter using ethidium bromide and fluorescein diacetate (Sigma-Aldrich), under fluorescence microscopy, were performed.

2.6 | Western blotting

Western blotting was applied to free or encapsulated hUCMS treated with or not with IFN-γ to evaluate the production of some immunomodulatory molecules at protein level. To this aim, protein samples (40 μg) were analyzed using 10% or 12% (v/v) sodium dodecyl sulfate-polyacrylamide gel electrophoresis and transferred onto nitrocellulose membranes (Bio-Rad Laboratories). The detection antibodies used were rabbit anti-human IDO1 (1:100; Thermo Scientific, LiStarFish, Milan, Italy), mouse anti-human HLA-G (4H84) (1:200; Santa Cruz Biotechnology, Milan, Italy), mouse anti-human TGFβ1 (TB21) (1:200; Santa Cruz Biotechnology, Milan, Italy), and mouse anti-human βtubulin (1:8000; Sigma-Aldrich, Milan, Italy). Immunodetection was performed using Clarity™ Western ECL Substrate (Bio-Rad Laboratories) following the vendor's recommendations.

2.7 | Immunocytochemistry

To verify whether microencapsulated hUCMS maintained the capacity to produce immunomodulatory molecules after in vivo permanence, immunocytochemistry was applied on microcapsules, upon their retrieval from NOD mice, treated with 3.7% PFA overnight at 4°C. Permeabilization was carried out with 0.01% Triton X-100 in D-PBS for 15 minutes and blocked with 1% BSA in D-PBS for 1 hour. Primary antibody (mouse anti-human IDO1, 1:50; mouse anti-human HLA-G, 1:50, Santa Cruz) was incubated overnight; thereafter, a secondary antibody (goat anti-mouse IgG FITC conjugated, Molecular Probes) was applied for 1 hour. Cell nuclei were counterstained with SlowFade Gold antifade reagent with DAPI (Molecular Probes). We acquired the images by a Nikon Eclipse Ci fluorescence microscope.

2.8 | Histological and immunohistochemical analyses

To evaluate the pancreatic morphological behavior of transplanted vs not transplanted mice, their organs underwent histological treatment with hematoxylin/eosin and anti-insulin staining. For histological analyses, the retrieved pancreatic samples underwent fixation in 10% neutral-buffered formalin for 24 h at room temperature,

dehydration, and paraffin embedding. The tissue samples were cut by a rotary microtome (3.5 μm thick slices) and the specimens stained with hematoxylin/eosin (H&E). Tissue staining followed standard histology protocols. Immunohistochemical analysis was performed on 3.5-μm-thick slides, using primary antibodies, specific for insulin. Automated immunohistochemistry employed the Leica BOND system (Leica Biosystems Newcastle Ltd, UK) on a Leica BOND-III instrument. The slides were counterstained with H&E. The preparations were examined under light microscopy (Nikon Eclipse Ci).

2.9 | Intraperitoneal graft of microencapsulated hUCMS: the NOD model

The encapsulated hUCMS (Cps/hUCMS) (2.5×10^6 cells in 1.3 mL of sodium alginate) were grafted intraperitoneally, into female NOD/MrkTac mice, purchased from Taconic Biosciences, Inc Under general anesthesia, 1.3 mL of microcapsules was deposited intraperitoneally into each mouse. The mice were housed and fed, under specific pathogen-free conditions. Autoimmune diabetes, on average, develops in 80% of NOD/MrkTac female mice by 24 weeks of age. The animals underwent BG monitoring, starting from the 10th week of birth. Glucose challenge tests were performed at 13 to 15 weeks. In particular, the IPGTT consisted of administering 2 mg of glucose g^{-1} body mass and measuring BG at 15, 30, 60, and 120 minutes post-treatment, after an initial assessment of fasting BG (16 h of overnight fast). All BG measurements were recorded using OneTouch Select Plus Glucometer (OneTouch, LifeScan, Inc). When IPGTT became abnormal, on at least two consecutive instances, the microencapsulated hUCMS TX was performed into two NOD mouse groups: (#1, "target window") n = 12, BG range 200-350 mg dL^{-1}; (#2, "out of window") n = 6, BG range 350-500 mg dL^{-1}. The transplanted mice were housed individually, with BG being monitored twice a week over the 216 days of TX period. Some animals were sacrificed shortly after transplantation, and in particular at 10 (n = 2) and 28 days (n = 2) of TX, for immunological and histological evaluations. The long-term remitters again underwent an IPGTT after 40 and 150 days of TX. Three NOD mice received empty microcapsule grafts and served as controls. NOD mice that had not become diabetic (n = 3), or became diabetic but did not undergo TX, served for additional controls (n = 3).The animals were euthanized by terminal anesthesia. We retrieved the microcapsules, upon laparotomy, by peritoneal lavage with saline, and placed them into sterile tubes. Following careful washing, to discard blood debris or peritoneal cells, the capsules were re-suspended in complete medium, and housed into culture flasks, at 37°C in 95% air/CO_2 for further analysis. After 24 h incubation, microcapsule aliquots were tested for cell viability, while the remainder was fixed for histology. The thymus, spleen, and lymph nodes, upon retrieval, were soaked in saline for subsequent cell phenotypic analysis. The removed pancreases underwent histological evaluations and Western blot analysis.

All the in vivo studies were conducted in compliance with national (Italian Approved Animal Welfare Assurance 512/2015 PR) and the University of Perugia Animal Care and Use Committee guidelines.

2.10 | Cell phenotypic analysis of lymphoid organs

We performed a phenotypic analysis of the T-cell subsets to clarify which cell populations would be subject to immunomodulation within the system. Cell phenotypic analysis was applied to the murine lymphoid organs after sacrifice. Thymus, spleen, and mesenteric lymph nodes underwent mechanical disruption to obtain a cell suspension. To identify T-cell subsets by flow cytometry (FC), we performed surface staining with FITC, phycoerythrin (PE), or allophycocyanin

(APC)-labeled anti-mouse CD4, CD25, and the respective isotype controls (MiltenyiBiotec). For the detection of Th1, Th2, Th17, and Treg transcription factors, the cells were processed with FoxP3 Staining Buffer Set (MiltenyiBiotec) and intracellular staining was performed using PE- or APC-labeled anti-mouse Tbet, GATA3, RORγt, FoxP3, and respective isotype controls (MiltenyiBiotec). Up to three fluorochromes applied to the same vial with the samples being analyzed by a FACSCalibur flow cytometer and CellQuestPro™ software (BD).
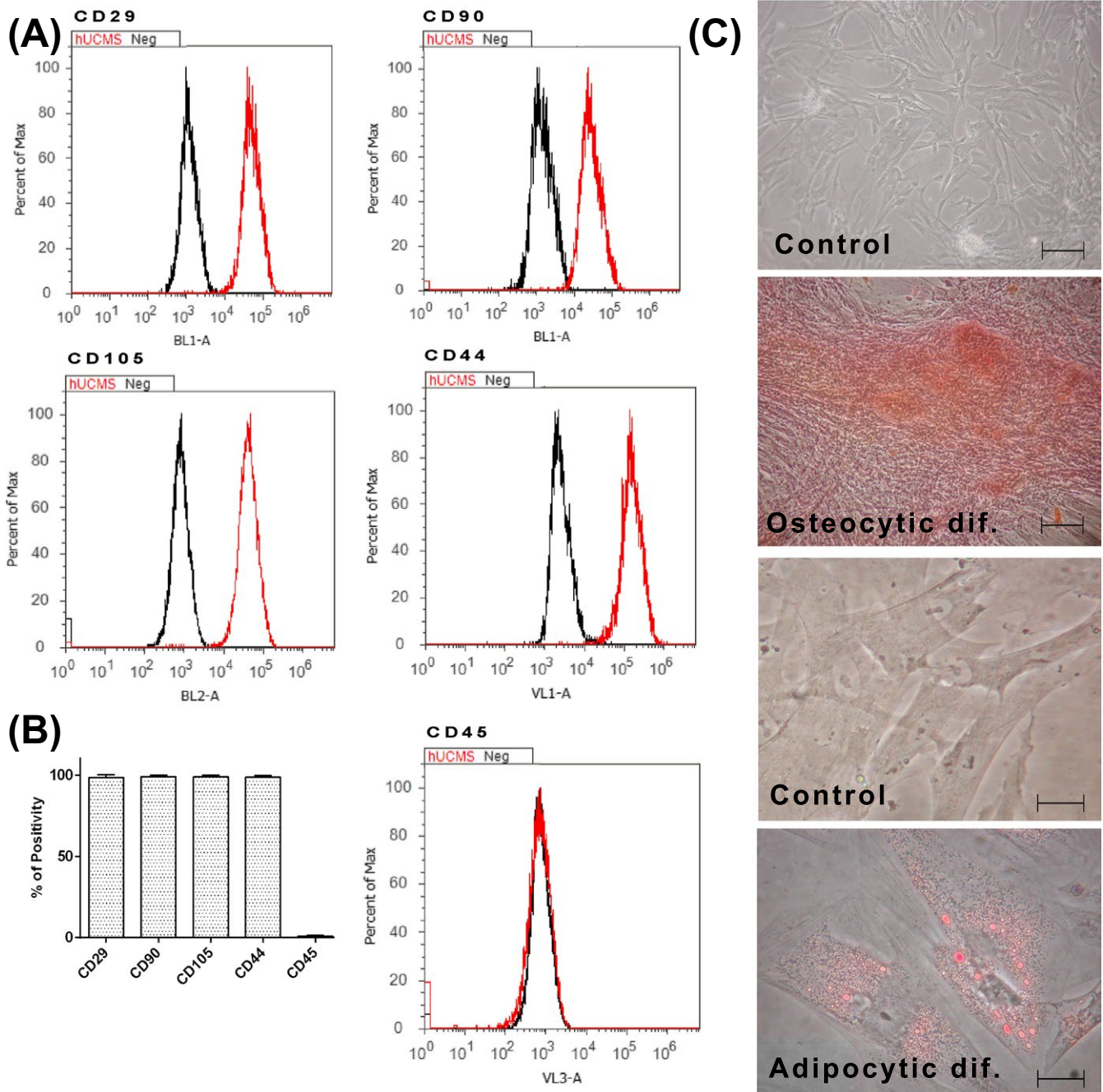

FIGURE 1 hUCMS characterization. A, Cytofluorimetric panel representative for the indicated markers. B, Average values for mesenchymal phenotype markers shown by hUCMS (n = 10). C, Osteocytic and adipocytic potential of hUCMS, as determined by staining with Oil-Red-O and Alizarin Red-S, respectively, after 3 weeks of specific induction. Magnification bars are 100 μm (osteocytic differentiation) and 10 μm (adipocytic differentiation)
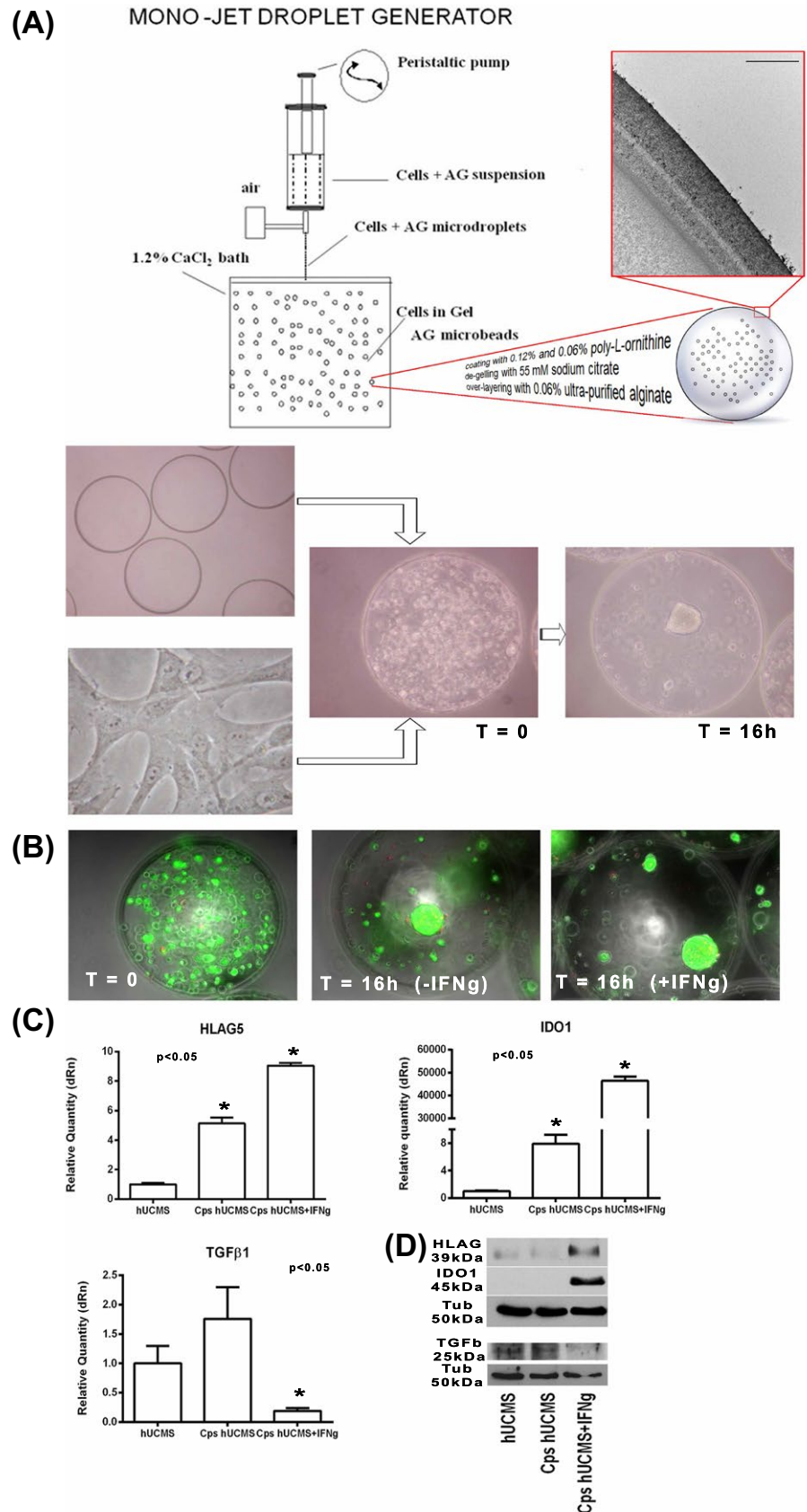
(A)

(B)

(C)

(D)

FIGURE 2 A, Schematic representation of the microencapsulation procedure with a TEM image of microcapsule wall. Magnification bar is 10 μm. Microencapsulated hUCMS are shown immediately and at 16 h after the encapsulation procedure. B, Viability of microencapsulated hUCMS was over 95%, and it was maintained after the treatment with IFN-γ. C, Representative qPCR for the indicated markers, performed on hUCMS, encapsulated hUCMS after pre-treatment or not with IFN-γ. (n = 3; $P < 0.05$). The expression of each marker, relative to not encapsulated hUCMS, equaled 1. HPRT1 was used for normalization. All results were representative of three independent experiments. D, Western blotting evaluation of IDO1, IL6, TGFβ1, and HLA-G proteins. All results are representative of three independent experiments

2.11 | Data analysis

For the in vivo experiments, survival data were analyzed by Kaplan-Meier plots. Paired data were assessed by Student's *t* test, and one-way analysis of variance was used for multiple comparisons. All in vitro determinations were expressed as mean ±standard deviation (SD) in at least three independent experiments and considered significant for *P* values <0.05. All statistical analyses were performed using Excel 2003 (Microsoft Corporation).

3 | RESULTS

3.1 | Characterization and differentiation potential of hUCMS

All hUCMS cell preparations underwent FC at III-IV culture passages. A panel of five markers, typical for mesenchymal cells, was employed, with special regard to the usually detectable (CD105, CD29, CD44, CD90) or usually absent (CD45) Ab markers. Figure 1A demonstrates that all hUCMS preparations were consistently negative for CD45 (a
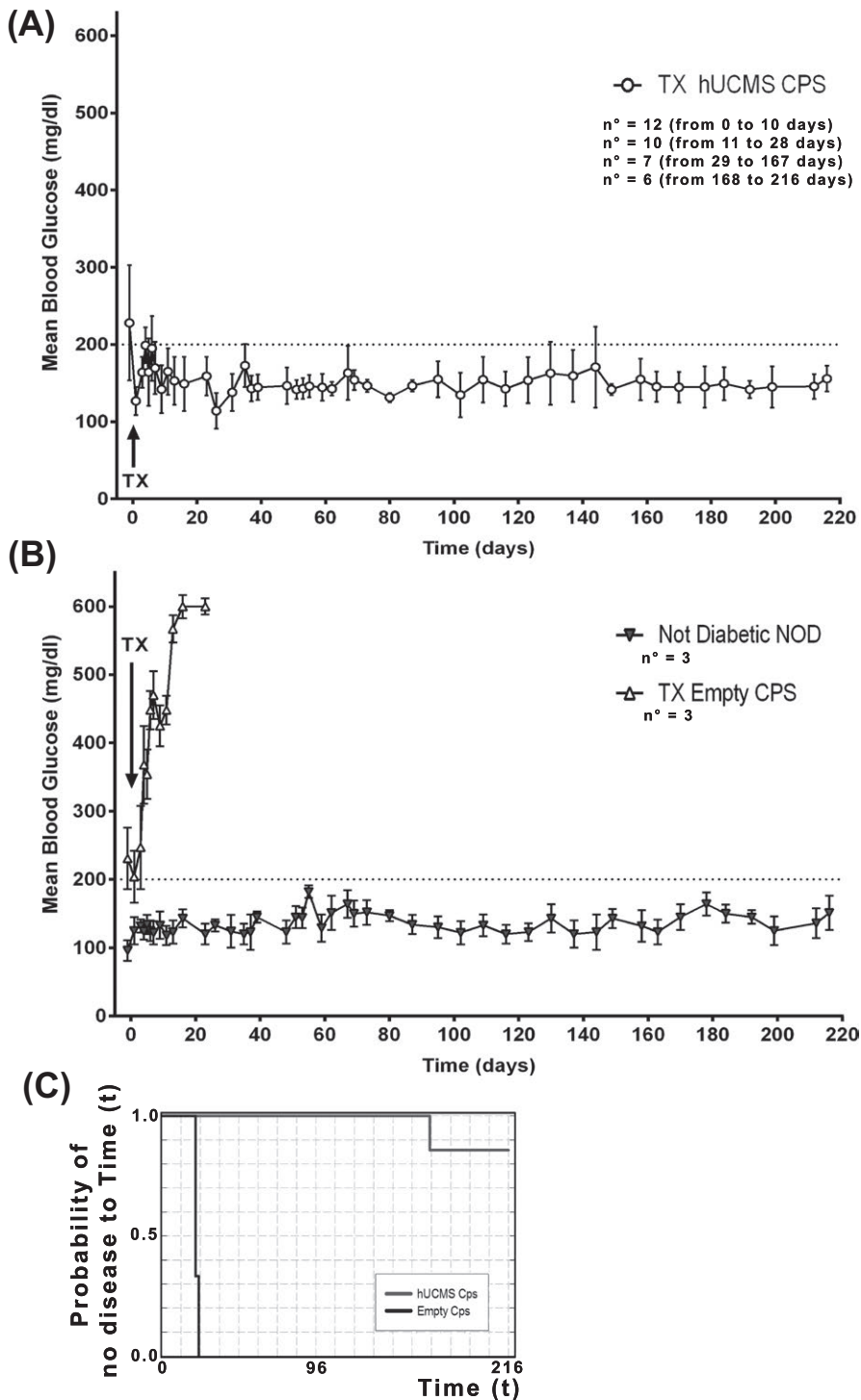

(A)

TX hUCMS CPS

n° = 12 (from 0 to 10 days)
n° = 10 (from 11 to 28 days)
n° = 7 (from 29 to 167 days)
n° = 6 (from 168 to 216 days)

(B)

Not Diabetic NOD
n° = 3

TX Empty CPS
n° = 3

(C)

hUCMS Cps
Empty Cps

FIGURE 3 A, Mean of random not fasting BG levels throughout 216 days of NOD mice transplanted with microencapsulated hUCMS. B, Mean of random not fasting BG levels of mice transplanted with empty capsules and not diabetic NOD mice. C, Kaplan-Meier survival plot: Diabetic female NODs were grafted with microencapsulated hUCMS or empty capsules, and survival probability was plotted over time. *P* < 0.001 for comparison between the two treatment groups was observed
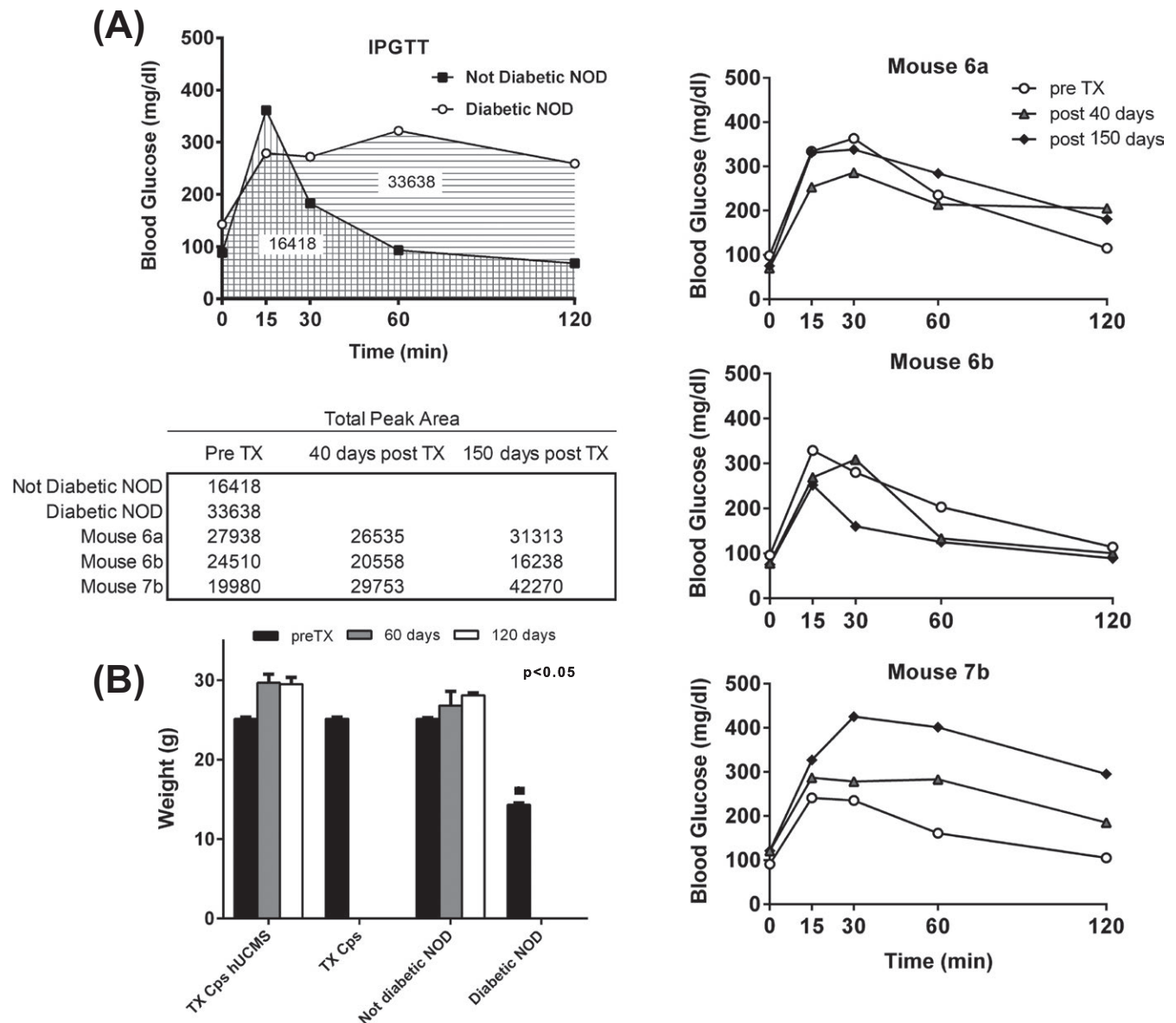
FIGURE 4 A, IPGTT of three representative NOD mice before transplantation, 40 and 150 d after transplantation with microencapsulated hUCMS in comparison with controls. B, Body weight of transplanted NOD over time in comparison with controls. *P < 0.05

typical hematopoietic marker) but clearly positive for CD29, CD90, CD44, and CD105. The expression of these markers was found in all preparations, and it never ranged below 98% (Figure 1B).

The obtained FC data clearly showed that our hUCMS[3] consisted of homogeneous, multipotent stromal mesenchymal cells. Furthermore, our cells were able to differentiate into adipogenic and osteogenic cell phenotypes upon incubation in "ad hoc" culture media (Figure 1C) that confirmed their identity as multipotent post-natal stem cells.

3.2 | Microencapsulation of hUCMS

hUCMS were embodied within ultrapurified, endotoxin-free sodium alginate microcapsules, with no viability loss. Microencapsulation

advantageously promoted cell aggregation into 3D spheroids that fully retained viability (Figure 2A, B). IFN-γ pre-treatment did not adversely affect cell viability (Figure 2B). IFN-γ increased hUCMS production of soluble molecules associated with immunoregulatory properties (Figure 2C, D).[20,22] In fact, after IFN-γ pre-treatment, IDO1 and HLA-G5 were strongly expressed. HLA-G1 was not expressed, while TGFβ1 mRNA was inhibited by IFN-γ after an initial increase. Western blots (Figure 2D) confirmed these observations.

3.3 | In vivo results of grafts into NOD mice

BG levels of NOD mice were monitored from the age of 10 weeks. In order to identify the target treatment window of early-stage diabetes, intraperitoneal glucose tolerance test (IPGTT) was performed at
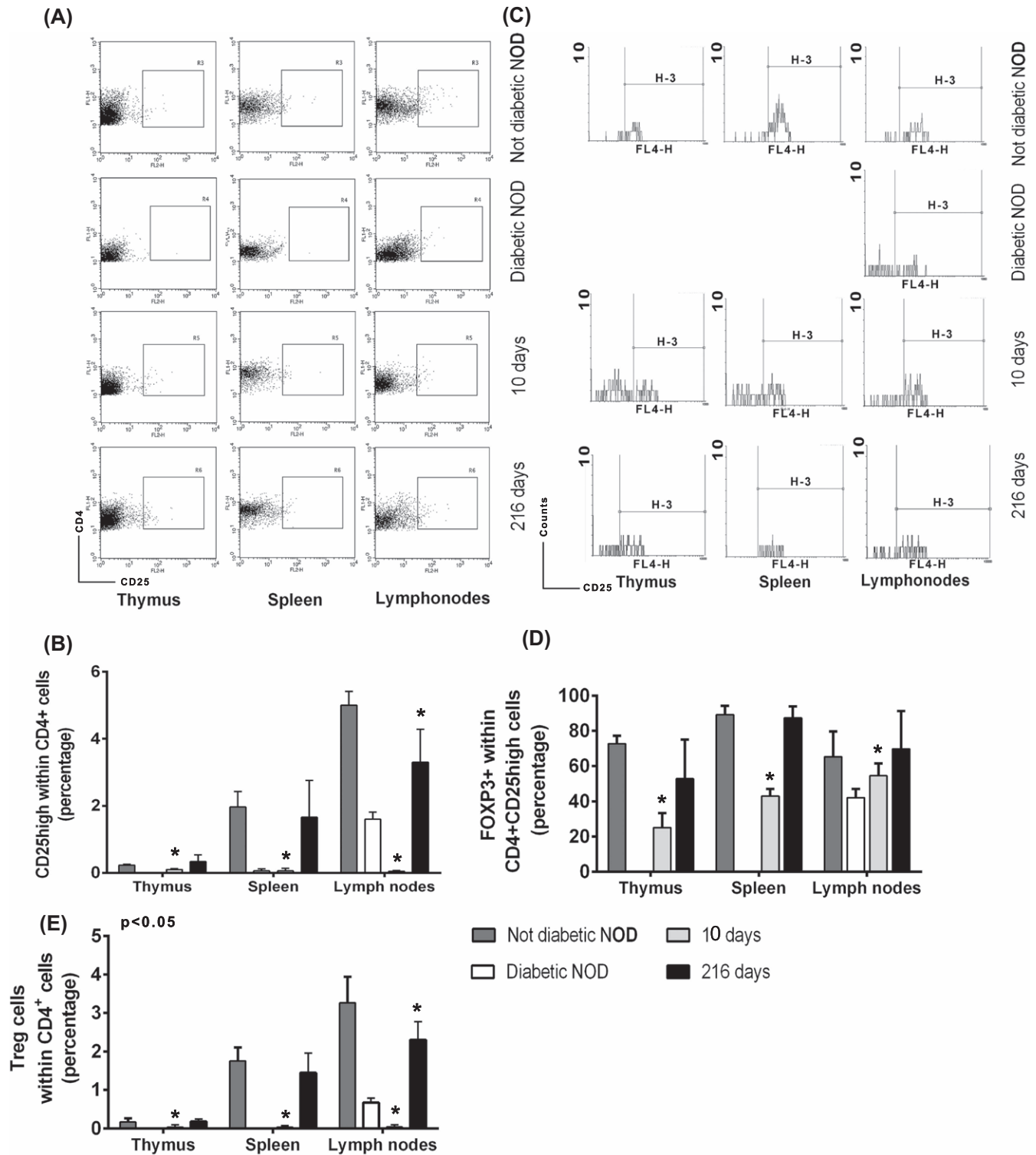
FIGURE 5 A, Dot plots (representative intact data) of cells from the indicated organs stained with anti-CD25 and anti-CD4 Abs. $CD4^+CD25^{high}$ cells are within rectangles; B, $CD25^{high}$ cells within $CD4^+$ cells (mean percentage) in thymus, spleen, and lymph nodes C, Histograms (representative intact data) of FOXP3 expression within $CD4^+CD25^{high}$ cells. Since $CD4^+CD25^{high}$ cells are not detectable in the thymus and spleen of diabetic NOD mice that were not transplanted, the corresponding histogram has not been drawn (no events in the gate) and the two empty spaces correspond to no bars in the histogram graph on D. D, $FOXP3^+$ cells within $CD4^+CD25^{high}$ cells: Results are graphically represented as bars. E, $CD4^+CD25^{high}FOXP3^+$ cells (Treg) within $CD4^+$ cells (mean percentage) in thymus, spleen, and lymph nodes. The expression of $FOXP3^+$ in the indicated organs, at 10 and 216 days post-transplantation of microencapsulated hUCMS, is shown in comparison with not diabetic NOD and recent-onset diabetic NOD. *$P < 0.05$ (comparison between transplanted NOD mice with recent-onset diabetic and not diabetic NOD mice, at level of thymus, spleen, and lymph nodes)

13-15 weeks of age. When IPGTT results appeared abnormal in two consecutive tests, with BG levels ranging on 200-350 mg dL^{-1}, the mice entered TX protocols.

Following these criteria to detect the "graft window," remission of hyperglycemia was achieved and sustained for 216 days of TX (Figure 3A). Only one recipient (mouse 3a) showed an increase in BG levels at day 156 and was sacrificed at day 167 of TX. Figure 3B depicts the analysis of untreated mice that did not develop diabetes and those of grafted NODs receiving empty capsules, which survived only for a few days. Figure 3C depicts the Kaplan-Meier plot exhibiting survival rates of each group. The graph showed that 85.7% of NODs grafted with microencapsulated hUCMS went on 216 days of TX against none of those treated with empty microcapsules.

Figure 4A depicts the IPGTTs of three representative NODs within the group treated with encapsulated hUCMS at 40 and 150 days, as compared with abnormal IPGTT, and one of a NOD that never developed DM (respective areas under the curve are shown). Looking at the IPGTTs, in some of the recipients, the BG levels progressively increased over time (mouse 7B), while in others (mouse 6A), the curves remained abnormal but flat; in others again (mouse 6B), after 150 d of TX, the curve greatly improved over time, and

it was comparable to that of not diabetic NODs. Hence, if all these animals remained euglycemic after graft throughout the study, the IPGTTs showed that some animals were on reduced insulin production and/or eventually on an insulin storage mode. The analysis of the BG levels following IPGTT supported this assumption: Mice 6a and 7b showed high BG that required up to 7 days, until reached pre-test values (Supplemental data).

Body weight of the grafted mice increased over time comparably to those that had never developed DM (Figure 4B).

3.4 | Ex vivo testing of transplanted NODs

Starting from the microencapsulated hUCMS-induced inhibitory action on T1D T cells, previously assessed in vitro,[21] here we performed a phenotypic analysis of the T-cell subsets, ex vivo, to determine which cell populations would undergo modulation within the system. Adult mesenchymal stem cells had proved able to upregulate FoxP3, the master transcription factor of Treg cells within CD4$^+$CD25^{high} T cells.

With respect to Treg cell levels, FOXP3$^+$ cells appeared and their levels increased in the thymus, spleen, and lymph nodes of mice
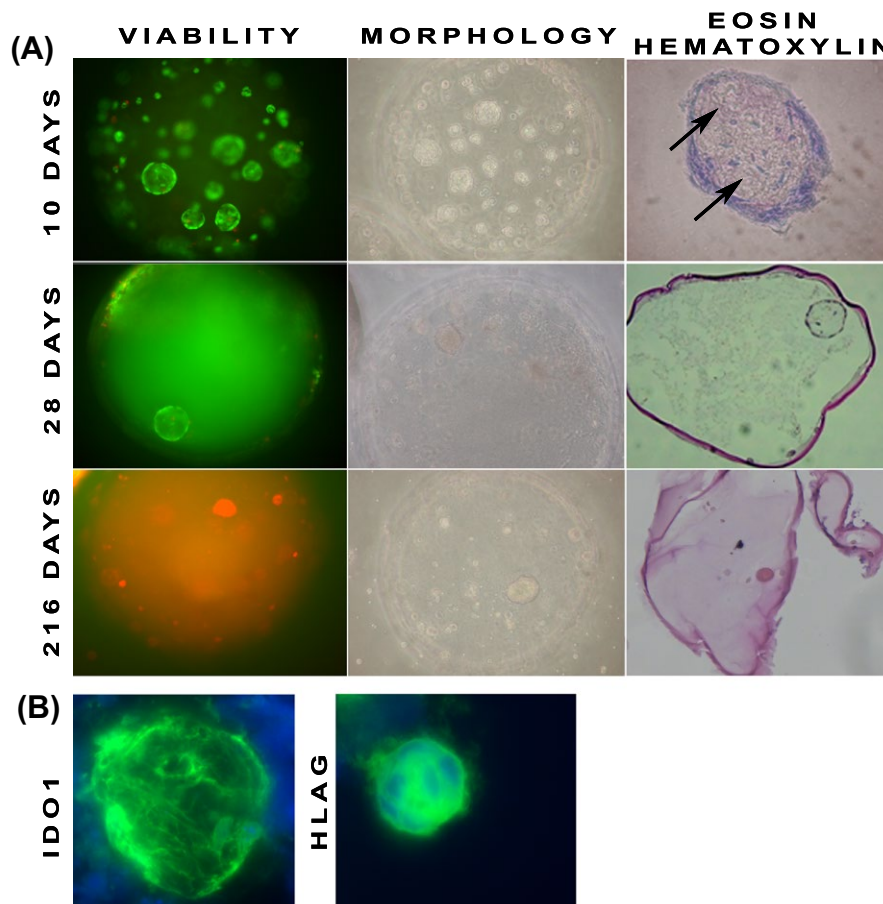

FIGURE 6 A, Morphology, morphological, and histological behavior of microencapsulated hUCMS retrieved from NOD mice at the indicated times. The conserved viability at short time after transplantation (10 and 28 days) and the competence to produce matrix proteins that filled the central aggregate core are evident (arrows). At 216 days after transplantation, the retrieved microcapsules show non-viable hUCMS. B, Immunofluorescence analysis for IDO1 and HLA-G of microencapsulated hUCMS aggregates retrieved at 10 days post-transplantation is shown
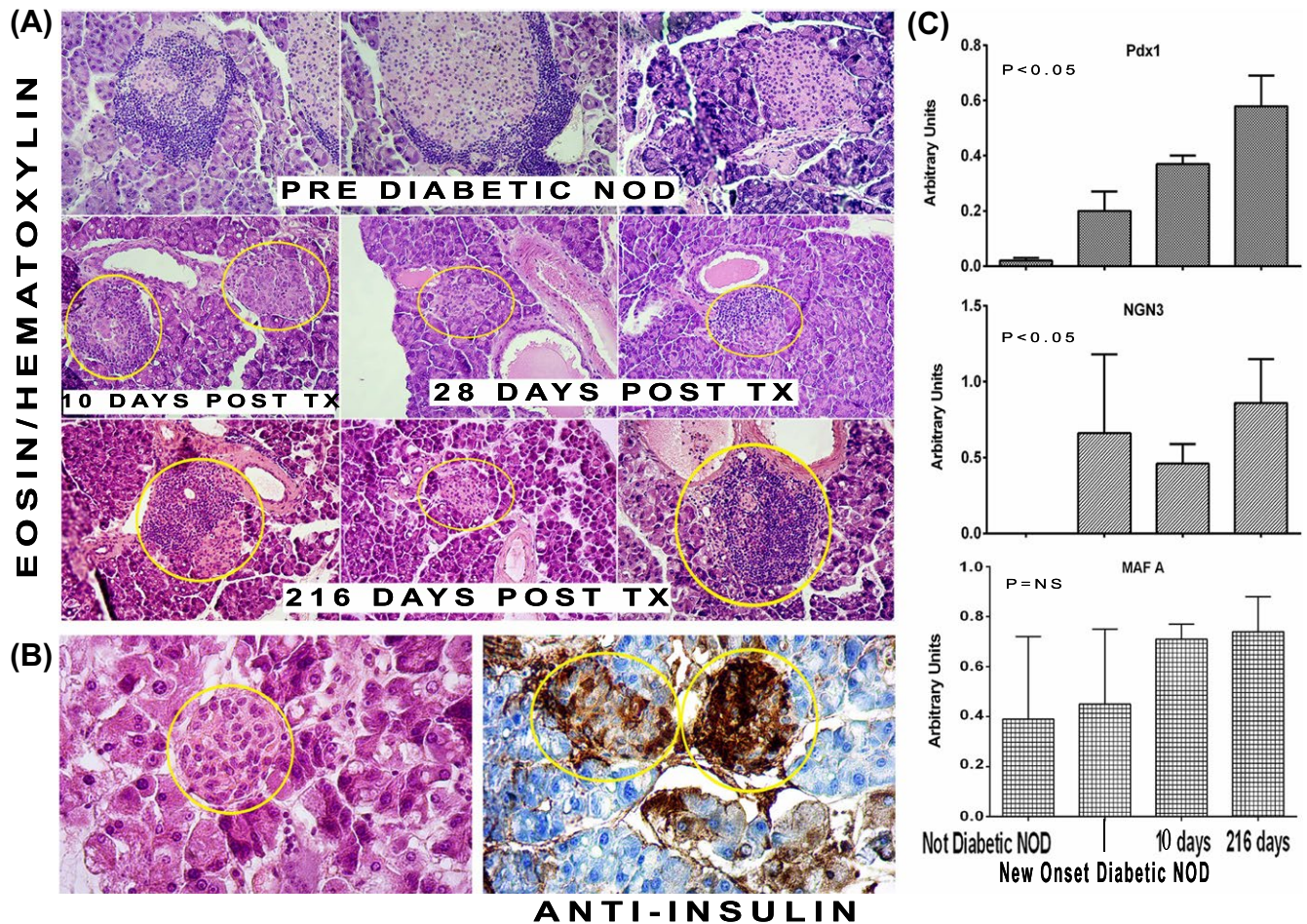
FIGURE 7 Histological examination of representative retrieved pancreases from treated NOD mice. A, Eosin hematoxylin staining of representative pancreases of pre diabetic NOD shows well-preserved islets, or with islets insulitis, or completely destroyed islets. Similar conditions are evident in pancreases from NOD mice transplanted with microencapsulated hUCMS sacrificed at different time points. Number of treated mice: pre-TX =2; 10 days =2; 28 days =2; 216 days =4. B, Well-preserved small islet is visible within the pancreas of NOD mice at 216 days on the left. On the right, the same islet stained with specific anti-insulin antibody. C, Western blotting analysis of pancreas for the indicated markers, at short- and long-term after transplantation, in comparison with untreated not diabetic NOD mice and untreated new-onset diabetic mice. Number of treated mice per group =2, except for the group of long-term remitters (216 d). The original Western blots are shown in Figure S3. *$P < 0.05$

treated with encapsulated hUCMS, at 10 days with a steady increase observed at longer time points following TX, as compared to untreated diabetic NOD mice (Figure 5). In fact, in untreated diabetic NOD mice, Treg cells were undetectable in both thymus and spleen. Remarkably, the proportion of the Treg cells in the lymphoid organs of transplanted mice, measured over longer time points, was comparable to those of the non diabetic control NODs.

At 10 days of TX, CD4$^+$CD25^{high} cells did not increase (Figure 5A, B): The few cells of this subset also expressed FOXP3, ranging on 50% (Figure 5C, D). However, at 216 days of TX, Treg cells raised in terms of both number and percentage (Figure 5C, D), since we observed an increase in both CD4+CD25^{high} and FOXP3$^+$ cells within them (Figure 5E).

Microcapsules retrieved at 216 days did not contain live cells, as expected, but they looked intact, with no surrounding inflammatory cells. On the contrary, microcapsules explanted at shorter time points post-TX (10-28 days post-TX) were associated with

viable embodied cells, appearing well-preserved morphologically (Figure 6A). Typically, upon microencapsulation, hUCMS tend to form 3D cell aggregates that synthesize their own extracellular matrix. This resulted in the distribution of cells in the periphery of the aggregate, while the core predominantly contained collagen (Figure 6A; Supplementary data). This behavior and arrangement permitted access to gas and nutrients for all cells within the spheroids, which prevented the formation of central necrotic cell cores. At 10 days post-TX, the microcapsules contained cell aggregates that were clearly positive for IDO1 and HLA-G, indicating a retention of viability and the functional competence of these cells.

The retrieved pancreases of the animals on remission of hyperglycemia, throughout 216 days of TX, and those of animals sacrificed at days 10 and 28, underwent histological examination (Figure 7A). At 216 days, pancreatic histology showed intact islets with no insulitis, or islets with insulitis or areas of cell infiltration, very similar to the immediate post-transplantation period. It is known that insulitis begins before

the onset of hyperglycemia and tends to decline with the progression of islets into fibrosis, when diabetes will become overt. Hence, an insulitis of comparable degree, between the two conditions, could indicate an arrest of the disease process.[23] Insulin staining was clearly identifiable in islets at 216 days post-TX (Figure 7B). Mouse 3a demonstrated a steep increase in BG at 156 days of TX, with subsequent sacrifice at 167 days, although an IPGTT performed at 150 days was still normal. The explanted pancreas, upon histology, showed small islets, devoid of inflammatory cell infiltration, although in this case, insulin expression was not present (Supplementary data). Possibly, IPGTT at 150 days could have functionally disabled still viable islet β-cells, although the mice exhibited normal BG levels. This may support the idea that islet cells of the grafted animals may work under basal conditions and under stress (IPGTT), but have no insulin storage required to recover after stress. The pancreases, retrieved at 10 days following TX and at the end of the study, were analyzed by WB, and were compared with those of animals that had not become diabetic, and to those with recent-onset diabetes. In general, in all grafted animals, we observed an increase in Pdx1 production in short-term analysis, and thereafter, as compared to not diabetic or recent-onset diabetic mice. Ngn3 was detectable only in the transplanted recipients, at the two selected time points, and in those with recent-onset diabetes. The latter indeed showed great variability as far as this protein expression was concerned. Ngn3 was undetectable in not diabetic mice. Differences in terms of MafA were not statistically significant, although individual differences between not diabetic and recent-onset diabetic, as compared to the two groups of transplanted mice, were evident (Figure 7C).

Islet regeneration depends on protein kinase A/signal transducer and activator of transcription 3 (PKA/STAT3) signaling-mediated NGN3 activation.[24] WB analysis on the retrieved pancreases, at short- and long-term post-TX, detected STAT3 protein, although in our experimental system we have not confirmed the presence of pSTAT3(TYR705) (data not shown). In fact, the treatment of animals with overt, established disease (BG 350-500 mg dL^{-1} for at least 1 wk) is destined to result in failure (Figure 8). In detail, the analysis of different time points after grafting of the various experimental conditions allowed us to recognize three main patterns. Some recipients remained hyperglycemic and rapidly worsened until sacrifice (type 2); others were severely hyperglycemic (500 mg dL^{-1}) until sacrifice at 32 days of TX (type 3). A third animal group showed a more peculiar behavior: Not fasting random BG values showed variable patterns, between frank hyperglycemia and euglycemia (type 1). Fasting BG partially clarified the metabolic behavior of these recipients: Those with stable hyperglycemia did not show decline of BG after fasting; those with variable BG responded to fasting with very low BG levels (30 mg dL^{-1}).

4 | DISCUSSION

We have shown that TX of microencapsulated hUCMS may enable restoration and long-term maintenance of normal BG levels in treated diabetic NOD mice. This outcome likely depends on
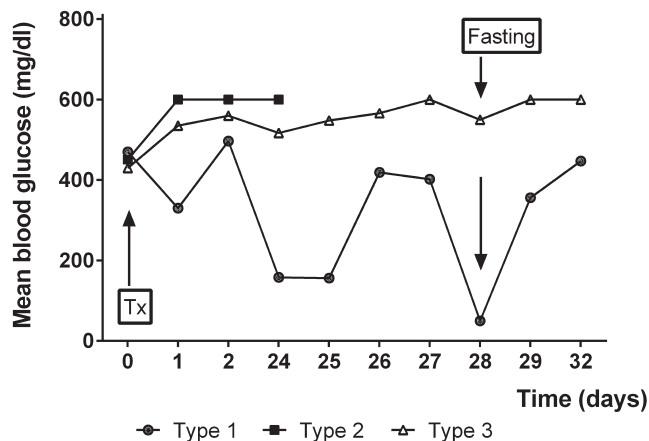

FIGURE 8 Random blood glucose levels of transplanted animals with overt, established diabetic disease. The three types of behavior are shown per single recipients

the action of microencapsulated hUCMS, which may only happen when TX occurs within a defined time window and modalities, within disease process. Over the past decade, growing evidence has demonstrated that hUCMS are not only multipotent cells with promising applications in regenerative medicine,[25] but also a powerful tool to modulate the immune system. Moreover, their availability is almost unlimited, and their efficient retrieval follows a rapid isolation process.[3] These cells can be cultured and expanded in vitro for at least five passages, with favorable impact on their number.

In terms of immunity, hUCMS may interact with the majority of immune cell types, via cell-to-cell contact. Such interaction leads to inhibition of effector T lymphocytes and stimulation of regulatory T cells (Treg).[26] Hence, hUCMS currently are used for the treatment of several autoimmune disorders, including, but not limited to, rheumatoid arthritis (RA).[27] However, cell-to-cell interactions deserve ad hoc reflections: In fact, we had observed that if hUCMS underwent direct contact with lymphocytes, isolated from patients with primary Sjögren's syndrome[6] or those with T1D,[21] their immunomodulatory potential was blunted. On the other hand, if physical contact between hUCMS and immune cells is prevented (ie, by microcapsules), immune activity of the cells is preserved, likely by release of soluble mediators.[28,29] To this end, microencapsulation within biocompatible materials, by providing a dynamic and immunoisolatory microenvironment, should be recommended.[29]

Here, we have demonstrated how microencapsulated hUCMS, upon overnight incubation with IFN-γ, significantly increased the expression of key soluble molecules, associated with both immunomodulatory properties, such as IDO1, and HLA-G5, an important tolerogenic player at the fetal-maternal interface that is deeply involved in immunoregulatory pathways.

Furthermore, this type of procedure does not require pre-graft immunosuppression, and it additionally allows cell TXs to function, as shown by our work, with no rejection events. Microencapsulation is associated with further advantages: It induces the formation of

cell aggregates, within a 3D architecture, that are particularly efficient in maintaining cellular viability in vitro and in vivo, for long periods of time.[20,21] Moreover, the procedure allows hUCMS to continue production of immunomodulatory molecules, namely IDO1 and HLA-G for at least the 28 days of TX. This all indicates that the hUCMS/microcapsule unit, rather than individual loose cells, by constituting an efficient drug delivery system, may represent a solid approach for the possible cure of autoimmune diseases. In our opinion, normalization of Treg cells at 216 d of graft does not mean that hUCMS mechanistically act through Treg. Treg recovery at the end of the study suggests that treatment with microencapsulated hUCMS has interrupted, directly or indirectly, progressive decline of Treg, as observed in the NOD mice with overt, severe diabetes thereby re-establishing balance of the immune system. Possible explanations to this outcome may be a) protection from apoptosis; b) maturation of pTreg (peripherally derived Treg) from conventional Tregs; increased Treg proliferation due to different microenvironment, exposure to different antigens, or other mechanisms. These different possibilities will be the subject of a specific study; c) Treg presence certainly contributed to protection of the mouse islet cells; and d) direct effects of hUCMS on islet cells have been reported by the literature, but these preliminary reports will require "ad hoc" designed study.[14,30]

We assumed that T1D treatment with immunomodulatory cells does not induce, per se and directly, remission of the disease unless a minimal, residual β-cell mass is present.[31] Thus, a key factor for the successful transplantation of microencapsulated hUCMS, and in general, of immunomodulatory cells, is represented by stage of the disease process. It is then critical a timely detection of time window, by random BG measurements both in fasting conditions and upon IPGTT.

In our experimental model, selection of the correct time window has proven to succeed, in terms of long-term survival and health preservation of the treated NODs. However, IPGTT indicated that the precise time window could be difficult to recognize in all animals. In fact, some animals exhibited glucose intolerance, which impaired return to euglycemia after the glucose load, or induced alterations of the curve itself. This leads us to believe that in the case of possible translation into humans, other diagnostic tools should apply for assessment of the residual islet β-cell mass (ie, intravenous glucagon test).

Previous reports seem to suggest that pancreatic endocrine regeneration does not occur by reactivation of specialized progenitors in adult tissues. On the contrary, differentiated pancreatic cells assume the status of optional precursors, under regenerative conditions, by either giving rise to newly formed β-cells or duplicating pre-existing β-cells.[31] The extent of the β-cell loss and environmental glucose conditions may play an important role in dictating the mode of β-cell replacement. Modest β-cell damage leads to creation of new β-cells, by self-duplication, while extensive endocrine tissue cell damage may induce activation of optional progenitors and their subsequent differentiation into new β-cells. In this scenario, reactivation of the embryonic pancreatic endocrine cell-specific gene NGN3, followed by an increase in Pdx1 and MafA, seems to be critical for sustained β-cell regeneration in most β-cell regeneration models so far reported.[31,32] The regeneration process is dependent on the protein kinase A/signal transducer and activator of transcription 3 (PKA/STAT3) signaling. Ngn3 activation seems to mediate this outcome.[24] Our data did not reveal the presence of protein pSTAT3 (TYR705). Hence, increase in Pdx1, NGN3, and MafA in the pancreas of short-term, but mainly long-term animals, could indicate retention/repair/replication of previously damaged islet cells rather than a true regeneration process. In light of these observations, we believe that graft timing of immunoregulatory stem cells (such as hUCMS) is a critical and limiting factor that may determine (or otherwise not) success of the intervention.

This graft series has confirmed our hypothesis, that treatment with immunomodulatory cells, does not induce remission of diabetes in the absence of a minimal residual mass of viable β-cell mass. In fact, such minimal residual β-cell mass, through the secretion of insulin, permits control of BG, thereby creating favorable environmental conditions, which improves their own survival and otherwise limited β-cell replication.[31]

These data are only apparently negative, in our opinion, as it clearly indicates that the pancreas of these transplanted animals was not severely damaged, a condition associated with regeneration phenomena.

An important aspect is to clarify whether microencapsulated hUCMS may directly affect the islet cells. Several growth factors, namely IGF, EGF family, lactogens, hepatocyte growth factor, glucagon-like peptide-1, and parathyroid hormone-related protein, have deemed to both stimulate rodent β-cell proliferation and improve cell survival in vitro and in vivo.[33,34] Moreover, cytokines, including members of the IL6, IL10, and IL27 families, regulate β-cell survival.[35] hUCMS produce many of the above cited molecules that could contribute on stimulating expansion of pre-existing β-cells.[36,37] Of course, this hypothesis will require "ad hoc" confirmatory studies.

Another potential advantage, associated with microencapsulated hUCMS, is the possibility of using relatively thin graft material. In fact, as shown by our previous in vitro experimental models of Sjögren syndrome and T1D, maximum efficacy of hUCMS in inhibiting proliferation of activated peripheral blood mononuclear cells (PBMCs) coincided with a dilution PBMC:hUCMS of 1:100.[6,20] The consequential significant reduction in required graft mass would permit access to multiple grafting procedures, if needed.

Overall, the presented data show that our experimental intervention may block the disease process associated with autoimmune DM in NOD mice. This results not in a cure but is prevents the onset of hyperglycemia, in these animals that closely mimic human T1D.

5 | CONCLUSIONS

We provided evidence that microencapsulated hUCMS grafts may successfully treat a strong animal model of spontaneous T1D like the NOD mouse. These cells, within microcapsules, comply with safety, efficacy, and stability requirements. In fact, as for safety, they did not transform nor did they require any host's immunosuppression.

As for efficacy, hUCMS induced a stable reversal of hyperglycemia in non obese diabetic (NOD) mice with recent-onset diabetes. Finally, as for durability, microencapsulated hUCMS permitted achievement of normal metabolic control in the grafted NODs over extraordinarily long periods of time (216 days post-TX).

In light of these pre-clinical results, it may be possible to speculate on translation of the obtained data to a phase 1 pilot clinical trial in patients with recent-onset T1D.

CONFLICT OF INTEREST

The authors approve the final article and declare that there is no conflict of interest with regard to the publication of this paper.

AUTHOR CONTRIBUTIONS

PM designed the research, performed experiments, analyzed data, wrote the paper, and arranged figures; TP performed experiments and analyzed data; AA performed experiments and analyzed data; OB performed experiments; GB designed the research, performed experiments, and wrote the paper; RC edited the paper and supervised experiments.

ORCID

Riccardo Calafiore https://orcid.org/0000-0002-7560-0081

REFERENCES

1. Couzin-Frankel J. Trying to reset the clock on type 1 diabetes. *Science*. 2011;333:819-821.
2. Mathieu C, Gillard P. Arresting type 1 diabetes after diagnosis: GAD is not enough. *Lancet*. 2011;378:291-292.
3. Montanucci P, Basta G, Pescara T, Pennoni I, Di Giovanni F, Calafiore R. New simple and rapid method for purification of mesenchymal stem cells from the human umbilical cord Wharton jelly. *Tissue Eng Part A*. 2011;17:2651-2661.
4. Bartholomew A, Sturgeon C, Siatskas M, et al. Mesenchymal stem cells suppress lymphocyte proliferation in vitro and prolong skin graft survival in vivo. *ExpHematol*. 2002;30:42-48.
5. Di Nicola M, Carlo-Stella C, Magni M, et al. Human bone marrow stromal cells suppress T-lymphocyte proliferation induced by cellular or nonspecific mitogenic stimuli. *Blood*. 2002;99:3838-3843.
6. Alunno A, Montanucci P, Bistoni O, et al. In vitro immunomodulatory effects of microencapsulated umbilical cord Wharton jelly-derived mesenchymal stem cells in primary Sjögren's syndrome. *Rheumatology (Oxford)*. 2015;54:163-168.
7. Sato K, Ozaki K, Oh I, et al. Nitric oxide plays a critical role in suppression of T-cell proliferation by mesenchymal stem cells. *Blood*. 2007;109:228-234.
8. Djouad F, Charbonnier LM, Bouffi C, et al. Mesenchymal stem cells inhibit the differentiation of dendritic cells through an interleukin-6-dependent mechanism. *Stem Cells*. 2007;25:2025-2032.
9. English K, Barry FP, Field-Corbett CP, Mahon BP. IFN-gamma and TNF-alpha differentially regulate immunomodulation by murine mesenchymal stem cells. *ImmunolLett*. 2007;110:91-100.
10. Xu G, Zhang L, Ren G, et al. Immunosuppressive properties of cloned bone marrow mesenchymal stem cells. *Cell Res*. 2007;17:240-248.
11. La Rocca G, Corrao S, Lo Iacono M, et al. Novel immunomodulatory markers expressed by human WJ-MSC: an updated review in regenerative and reparative medicine. *Open Tissue Eng Regener Med J*. 2012;5:50-58.
12. Selmani Z, Naji A, Zidi I, et al. Human leukocyte antigen-G5 secretion by human mesenchymal stem cells is required to suppress T lymphocyte and natural killer function and to induce CD4+CD25highFOXP3+ regulatory T cells. *Stem Cells*. 2008;26:212-222.
13. Li L, Davidovich AE, Schloss JM, et al. Neuronal lineage differentiation of embryonic stem cells within alginate microbeads. *Biomaterials*. 2011;32:4489-4497.
14. Gnecchi M, Danieli P, Malpasso G, Ciuffreda MC. Paracrine mechanisms of mesenchymal stem cells in tissue repair. *Methods Mol Biol*. 2016;1416:123-146.
15. Trouche E, GirodFullana S, Mias C, et al. Evaluation of alginate microspheres for mesenchymal stem cell engraftment on solid organ. *Cell Transplant*. 2010;19:1623-1633.
16. Calafiore R, Basta G, Luca G, et al. Standard technical procedures for microencapsulation of human islets for graft into nonimmunosuppressed patients with type 1 diabetes mellitus. *Transplant Proc*. 2006;38:1156-1157.
17. Murua A, Portero A, Orive G, et al. Cell microencapsulation technology: towards clinical application. *J Control Release*. 2008;132:76-83.
18. deVos P, Andersson A, Tam SK, et al. Advances and barriers in mammalian cell encapsulation for treatment of diabetes. *ImmunolEndocrMetabol Agents Med Chem*. 2006;6:139-153.
19. Thanos CG, Calafiore R, Basta G, et al. Formulating the alginate-polyornithine biocapsule for prolonged stability: evaluation of composition and manufacturing technique. *J Biomed Mater Res A*. 2007;83:216-224.
20. Montanucci P, Pennoni I, Pescara T, et al. The functional performance of microencapsulated human pancreatic islet-derived precursor cells. *Biomaterials*. 2011;32:9254-9262.
21. Montanucci P, Alunno A, Basta G. Restoration of t cell substes of patients with type 1 diabetes mellitus by microencapsulated human umbilical cord Wharton jelly-derived mesenchymal stem cells: an in vitro study. *Clin Immunol*. 2016;163:34-41.
22. Basta G, Calafiore R. A process for the ultrapurification of alginates. Patent number: WO 2009093184 A1.

23. Afelik S, Rovira M. Pancreatic β-cell regeneration: advances in understanding the genes and signaling pathways involved. *Genome Med.* 2017;9:42-50.

24. Valdez IA, Dirice E, Gupta MK, et al. Proinflammatory cytokines induce endocrine differentiation in pancreatic ductal cells via STAT3-dependent NGN3 activation. *Cell Rep.* 2016;15:460-470.

25. Barry F, Murphy M. Mesenchymal stem cells in joint disease and repair. *Nat Rev Rheumatol.* 2013;9:584-594.

26. Mattar P, Bieback K. Comparing the immunomodulatory properties of bone marrow, adipose tissue, and birth-associated tissue mesenchymal stromal cells. *Front Immunol.* 2015;6:560-565.

27. Liu Y, Mu R, Wang S, et al. Therapeutic potential of human umbilical cord mesenchymal stem cells in the treatment of rheumatoid arthritis. *Arthritis Res Ther.* 2010;12:R210.

28. Deng D, Zhang P, Guo Y, Lim TO. A randomized double-blind, placebo-controlled trial of allogeneic umbilical cord-derived mesenchymal stem cell for lupus nephritis. *Ann Rheum Dis.* 2017;76:1436-1439.

29. Alunno A, Bistoni O, Montanucci P, et al. Umbilical cord mesenchymal stem cells for the treatment of autoimmune diseases: beware of cell-to-cell contact. *Ann Rheum Dis.* 2018;77:e14.

30. Bell GI, Meschino MT, Hughes-Large JM, et al. Combinatorial human progenitor cell transplantation optimizes islet regeneration through secretion of paracrine factors. *Stem Cells Dev.* 2012;21:1863-1876.

31. Cavelti-Weder C, Li W, Zumsteg A, et al. Hyperglycaemia attenuates in vivo reprogramming of pancreatic exocrine cells to beta cells in mice. *Diabetologia.* 2016;59:522-532.

32. Wang S. Sustained Neurog3 expression in hormone-expressing islet cells is required for endocrine maturation and function. *PNAS.* 2009;106:9715-9720.

33. Baeyens L, Lemper M, Leuckx G, et al. Transient cytokine treatment induces acinar cell reprogramming and regenerates functional beta cell mass in diabetic mice. *Nat Biotechnol.* 2014;32:76-83.

34. Rooman I, Bouwens L. Combined gastrin and epidermal growth factor treatment induces islet regeneration and restores normoglycaemia in C57Bl6/J mice treated with alloxan. *Diabetologia.* 2004;47:259-265.

35. De Groef S, Renmans D, Cai Y, et al. STAT3 modulates β-cell cycling in injured mouse pancreas and protects against DNA damage. *Citation: Cell Death Dis.* 2016;7:e2272.

36. Benthuysen JR, Carrano AC, Sander M. Advances in β cell replacement and regeneration strategies for treating diabetes. *J Clin Invest.* 2016;126:3651-3660.

37. Gao X. Bone marrow mesenchymal stem cells promote the repair of islets from diabetic mice through paracrine actions. *Mol cell Endocrinol.* 2014;388:41-50.

SUPPORTING INFORMATION

Additional supporting information may be found online in the Supporting Information section at the end of the article.